

Intermetallic bonds and midgap interface states at epitaxial Al/GaAs(001) junctionsT. Maxisch,¹ N. Bingeli,² and A. Baldereschi¹¹*Institute of Theoretical Physics, École Polytechnique Fédérale de Lausanne, CH-1015 Lausanne, Switzerland*²*International Center for Theoretical Physics (ICTP), Strada Costiera 11, 34014 Trieste, Italy*

(Received 20 November 2002; published 26 March 2003)

Using first-principles pseudopotential calculations, we have investigated the nature of the electronic states with energies within the semiconductor band gap of abrupt, defect-free As-terminated Al/GaAs(001) junctions. While bondinglike/antibondinglike semiconductor evanescent states occur near the valenceband/conduction-band edges, the semiconductor midgap region is characterized by a different type of electronic states, not accounted for by commonly accepted models. These states, which correspond to intermetallic bonds between the outermost Ga cations of the semiconductor and Al atoms of the metal occur near the Fermi energy. They are localized at the interface and are located around the J point of the Brillouin zone. These new interface states derive from an interaction between localized states of the Al(001) surface and bulk GaAs conduction-band states, mediated by localized states of the unreconstructed As-terminated GaAs(001) surface.

DOI: 10.1103/PhysRevB.67.125315

PACS number(s): 73.20.-r

I. INTRODUCTION

Interfacial states with energy within the semiconductor fundamental band gap are known to play a major role in determining the Schottky barrier and transport properties of metal/semiconductor junctions.¹ Despite their importance, detailed theoretical investigations of these states, their nature, and formation mechanisms have been carried out in a few cases only. Recently, localized interfacial-gap states originating from frustrated bonds at metal/semiconductor junctions have been predicted theoretically for several epitaxial silicide-silicon² interfaces and for the Au/GaAs(001) contact.³

In the case of epitaxially grown Al/Ga_xAl_{1-x}As(001) junctions, experimental studies of the Schottky barrier dependence on hydrostatic pressure, temperature, and alloy composition x , brought about the interesting idea that the behavior of the Schottky barrier in these systems may be controlled by midgap interfacial states with a bonding character.^{4,5} This, together with the fact that *ab initio* calculations for defect-free Al/Ga_xAl_{1-x}As(001) junctions describe well the measured Schottky barrier trends,⁶ motivated us to investigate the nature of midgap interfacial states in defect-free epitaxial Al/GaAs(001) junctions.

Until now, no intrinsic localized interface state with energy within the semiconductor band gap has been predicted for Al/Ga_xAl_{1-x}As junctions. Earlier studies³ have shown that localized interface states occur several eV below the Fermi energy, in the lower portion of the valence band. Using a microscopic approach based on *ab initio* calculations, we show that localized interface states and resonances of a different type occur near the Fermi energy in defect-free epitaxial, As-terminated Al/GaAs(001) junctions. These states correspond to Al-Ga intermetallic bondinglike states that form across the junction. We investigate the mechanism responsible for the formation of these interface states, and show that they are related to localized states of the isolated Al and GaAs surfaces.

II. METHODOLOGY

The *ab initio* calculations are performed within the density-functional-theory framework using the local-density approximation (LDA). We employ a plane-wave basis set and Troullier-Martins pseudopotentials⁷ in the Kleinman-Bylander (KB) nonlocal form.⁸ The pseudopotentials are generated from the ground-state configuration of the spin unpolarized atoms, using the following core cutoff radii: $r_s = r_p = 2.2a_0$, $r_d = r_f = 2.7a_0$ for As and Ga, and $r_s = r_p = r_d = 2.2a_0$ for Al. We treat the Ga three-dimensional electrons as core electrons. For the KB form, we use as local component the f potential for Ga and As, and the d potential for Al.

The Al/GaAs(001) interface is modeled using a slab geometry in a supercell⁹ containing 13 atomic layers of GaAs and 23 atomic layers of Al, i.e., a total of 59 atoms and 191 electrons. The Al fcc lattice is rotated by 45° about the [001] growth axis with respect to the cubic lattice of GaAs in order to satisfy the epitaxial condition $a_{\text{Al},\parallel} = a_{\text{GaAs}}/\sqrt{2}$, where a_{GaAs} and $a_{\text{Al},\parallel}$ are the GaAs-bulk-equilibrium and Al in-plane lattice constants, respectively. A similar epitaxial geometry was used previously to model Al/Ga_xAl_{1-x}As(001) junctions,^{6,10} and is known to correspond to experimentally observed quasiepitaxial Al/GaAs(001) structures.^{11,12} Experimentally (and also in the *ab initio* calculations), the bulk-equilibrium lattice constant of Al is about 1% larger than $a_{\text{GaAs}}/\sqrt{2}$. Following macroscopic elasticity theory (MET), the Al in-plane compressive strain is accommodated by a 2% expansion of the Al overlayer along the growth direction in pseudomorphic structures. In this study, we use the theoretical value of the GaAs equilibrium lattice constant $a_{\text{GaAs}} = 5.52 \text{ \AA}$ and, following MET, we use $a_{\text{Al},\perp} = 4.06 \text{ \AA}$ for the strained Al slab.

The atomic structure of the abrupt As-terminated interface considered in this work is illustrated in Fig. 1. This structure corresponds to the lowest-energy configuration obtained by rigidly translating the Al slab relative to the GaAs slab and parallel to its surface.¹⁰ The equilibrium interfacial distance is $d_0 = 1.7 \text{ \AA}$ (see Fig. 1). At equilibrium, the volume of the supercell is $\Omega_0 = 6657a_0^3$. In the course of this study, we will

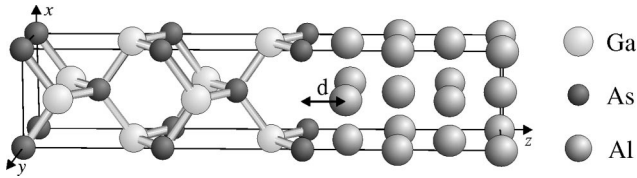


FIG. 1. Atomic structure of the abrupt, As-terminated Al/GaAs(001) interface. The x and y axes are rotated by 45° with respect to the conventional cubic axis of the semiconductor. The interfacial distance d measures the spacing between the As and Al layers at the junction.

also consider values of the interfacial distance d larger than d_0 . In such calculations, the atomic structures of the Al and GaAs slabs are kept frozen and only the interslab spacing is modified.

The symmetry point group of the Al/GaAs(001) interface is C_{2v} ,¹³ and the space group is symmorphic. The two-dimensional (2D) Brillouin zone (BZ) of the interface is shown in Fig. 2, where, for comparison, we also show the BZ's of the GaAs(001), Al(001) $c2 \times 2$ and Al(001) 1×1 surfaces. The latter one (one atom per unit cell) corresponds to the common description of the Al(001) surface, while the Al(001) $c2 \times 2$ configuration (two atoms per unit cell) is the relevant one in our interface study. We note that the BZ of the supercell, which is used in this study to model the interface, is three dimensional. However, its dimension along the k_z axis is very small in view of the large size of the supercell in this direction. Therefore, the electronic structure in the basal plane ($k_z=0$) of the 3D-BZ of the supercell provides a good description of the electronic structure in the whole BZ. In the supercell, the two As-terminated semiconductor sur-

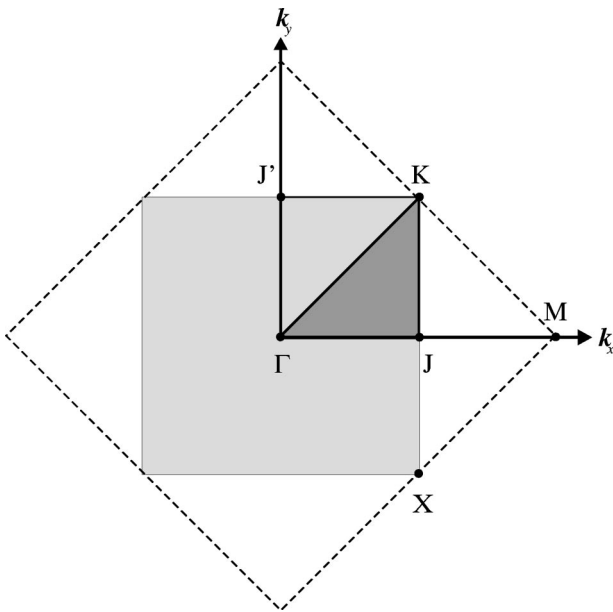


FIG. 2. Brillouin zone of the Al/GaAs(001) interface (gray square) and of the Al(001) 1×1 surface (dashed lines). The gray square is also the BZ of the isolated GaAs(001) and Al(001) $c2 \times 2$ surfaces. The irreducible part of the supercell BZ in the basal plane ($k_z=0$) is indicated by the dark triangle.

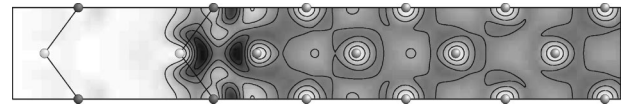


FIG. 3. Contour plot, in the basal plane including interfacial Ga, As, and Al atoms, of the integrated probability density of all electronic states with energy in the range $[E_F - 0.25 \text{ eV}, E_F + 0.25 \text{ eV}]$. Contour spacing is $3 \times 10^{-3} e/a_0^3$.

faces are equivalent to each other through a reflection with respect to the middle plane of the GaAs slab, followed by a 90° rotation around the $[001]$ axis ($x \rightarrow -y, y \rightarrow x, z \rightarrow -z$). This additional symmetry of the supercell, which does not apply to an isolated interface, reduces the irreducible part of the supercell BZ in the basal plane to one half of that of the 2D-BZ of the isolated interface.

In order to display on a common energy scale the Al/GaAs(001) interface-band structure and the projected band structures (PBS) of bulk Al and GaAs, which are obtained from separate calculations, we evaluate the shifts of the Al and GaAs electrostatic supercell potentials, relative to the mean value of the potential in the supercell, using the macroscopic average technique.⁹ This approach provides more precise energy lineups than direct alignment of exposed reference levels, e.g., ground-state or valence-band-edge energies from different systems.

The supercell calculations are performed with a kinetic-energy cutoff of 16 Ry for the plane-wave basis and using a (6,6,2) Monkhorst-Pack¹⁴(MP) k -point grid. Bulk computations for Al and GaAs are performed using a four-atom tetragonal unit cell with a kinetic-energy cutoff of 40 Ry and a (16,16,16) MP grid. The Fermi energy E_F of the metallic systems is determined using a Gaussian electronic-level broadening scheme¹⁵ with a standard deviation of 0.01 Ry. With these parameters, the numerical convergence of the electronic energies is $\sim 0.05 \text{ eV}$. The overall uncertainty on the interface-state energies relative to E_F , which is mainly attributed to the neglect of many-body effects within the LDA, is estimated as $\sim 0.1 \text{ eV}$.

III. RESULTS AND DISCUSSION

We have examined the probability density of electronic states with energy in the range $[E_F - 1.5 \text{ eV}, E_F + 1.5 \text{ eV}]$. For energies near the GaAs valence-band edge, i.e., about 1 eV below the Fermi energy, we find semiconductor bonding-like evanescent states at the interface. Conversely, at energies of about $E_F + 1 \text{ eV}$, i.e., near the conduction-band edge, semiconductor evanescent antibondinglike states occur. The behavior of such states is generally consistent with Tersoff's model description of the metal-induced gap states.¹⁶

In the midgap region, instead, the electronic states are of a different nature. In Fig. 3, we display, in the basal plane containing the interfacial Al and As atoms, the contour plot of the integrated probability density of all electronic states with energy in the range $[E_F - 0.25 \text{ eV}, E_F + 0.25 \text{ eV}]$. They amount to 11.15 electrons per supercell. The probability density assumes particularly large values near the interfacial Al atom as well as near the Ga cation closest to the interface

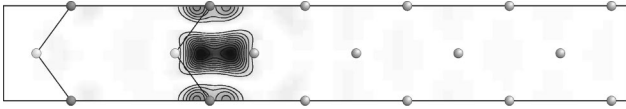


FIG. 4. Contour plot of the probability density of the localized interface state at the \mathbf{J} point of the 2D-BZ. Same plane and contour spacing as in Fig. 3.

(second semiconductor layer from the metal) indicating a Ga-Al intermetallic bonding structure. The probability density is also high on the As atom terminating the semiconductor slab, where the contours are similar to those of a dangling-bond surface state. The behavior of the probability density in the midgap region does not correspond to that expected for semiconductor bonding or antibonding states, which are predicted by Tersoff's model. Rather, it indicates the existence of interface states of a new type.

Investigation of the single-state contributions to the integrated probability density shown in Fig. 3, which derives from different regions of the BZ, indicates that the intermetallic bonding feature at the interface mostly comes from electronic states near the \mathbf{J} point of the BZ. Inspection of the charge density of individual electronic states at \mathbf{J} reveals an interface state with energy $E_F - 0.2$ eV which is fully localized at the junction. The contour plot of the probability density of this state is displayed in Fig. 4. It shows an Al-Ga intermetallic bonding structure which is clearly related to the high-probability-density feature observed at the interface (see Fig. 3). We note that the bond length of this structure is about 3 Å, which is quite remarkable since it is almost a factor 2 larger than the average interatomic bond length in covalent solids.

In Fig. 5, we show the Al/GaAs(001) interface band structure calculated in the supercell ($k_z = 0$), along the high symmetry lines Γ - \mathbf{J} - \mathbf{K} of the BZ. The electronic bands are displayed in an energy window covering the GaAs band gap. The bulk PBS's of GaAs and of Al (strained) are also shown in this figure. The Al PBS fills up almost entirely the semiconductor gap region, leaving only a small common gap near the \mathbf{J} point for energies in the range from $E_F - 0.7$ eV to

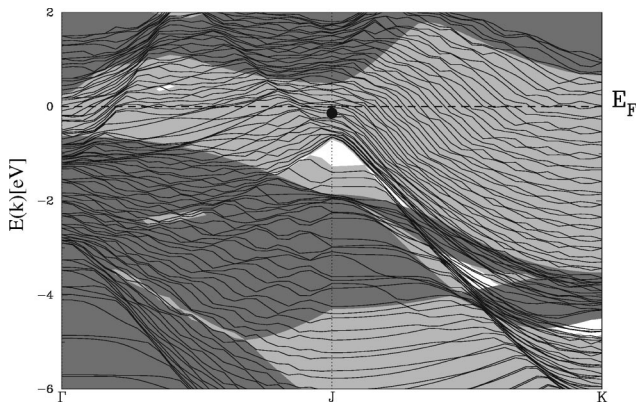


FIG. 5. Electron band structure of the Al/GaAs(001) interface. The solid point indicates the localized interface state at \mathbf{J} . The projected band structures of bulk GaAs (dark gray) and of epitaxially strained bulk Al (light gray) on GaAs(001) are also indicated.

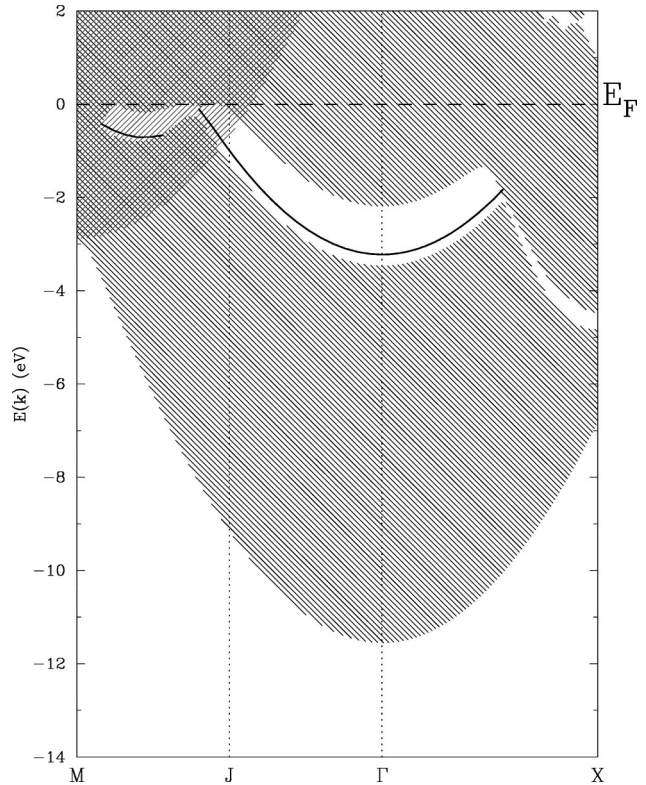


FIG. 6. Dispersion of the localized surface states of the epitaxially strained Al(001) surface along high-symmetry lines of the surface BZ. The left(right)-hatched area shows the projection of epitaxially strained Al bulk states which are even (odd) with respect to the mirror plane parallel to the relevant high-symmetry line and orthogonal to the surface.

$E_F - 1.3$ eV. The localized interface state at \mathbf{J} occurs at a higher energy, and is indicated by the solid point in Fig. 5. This state is clearly degenerate with electronic states of bulk Al, and its localization is made possible only by a different symmetry from that of the surrounding bulk continuum. We note that such a situation is actually known to occur in the case of the surface state of Al(001) for energies in the range from $E_F - 0.5$ eV to $E_F - 1$ eV.^{17,18} In our case, we find that, as in the case of the Al(001) surface state,^{17,18} the localized state at \mathbf{J} is even with respect to the σ_v reflection in the zx plane (see Fig. 4), whereas Al bulk states with similar energies at \mathbf{J} are odd with respect to σ_v (see Fig. 6). Thus, similarly to the case of the Al surface state, the Al/GaAs interface state cannot mix with electronic states of the Al bulk continuum and remains localized. The above similarities, together with the As dangling-bond surface structure appearing in the probability density of Fig. 3, suggest that localized states of the isolated Al(001) and GaAs(001) surface might be relevant for understanding the nature of the Al/GaAs(001) interface state.

In order to better understand the metal and semiconductor surface contributions to the localized interface state, we have studied the energies of the electronic states in the supercell as a function of the interfacial distance d , from its equilibrium value d_0 up to the value $d = 15a_0$, where the Al and GaAs surfaces are essentially noninteracting. This allows us to un-

ambiguously identify the dominant metal and semiconductor contributions as well as the interaction mechanism responsible for the formation of the interface state. As mentioned before, the atomic configurations of the Al and GaAs slabs are kept frozen, while increasing d , i.e., for large values of d we obtain an artificial unreconstructed GaAs slab and a strained metallic Al slab with their (001) surfaces. As a first step, we decided to study the electronic structure of such frozen slab surfaces.

The surface of the strained Al(001) slab was studied using a supercell including 41 layers of Al and nine equivalent vacuum layers. Such a thick Al slab was used to ensure negligible interactions between the two slab surfaces. The Al(001) surface state is indeed characterized by a very slow decay within the bulk material (decay length of $\sim 20 \text{ \AA}$).¹⁸ The Al slab calculations were carried out with a 32-Ry cutoff and using a (6,6,2) MP grid.

Figure 6 shows the PBS of the strained Al bulk along the Γ - \mathbf{J} - \mathbf{M} and Γ - \mathbf{X} high-symmetry lines of the Al 1×1 surface BZ. In this figure, we distinguish by different shadings the states which are even or odd relative to the vertical mirror plane which is parallel to the relevant high-symmetry line, i.e., the σ_v reflection along Γ - \mathbf{J} - \mathbf{M} and a σ_d reflection along \mathbf{G} - \mathbf{X} . A stomach gap is present below the Fermi energy for Al bulk states with even symmetry. At \mathbf{J} the gap extends from $E_F - 1.2 \text{ eV}$ to E_F . In the stomach gap, we show the dispersion of the Al(001) surface state with the same (even) symmetry. Along the \mathbf{J} - \mathbf{M} segment, the surface state becomes degenerate with Al bulk states with odd symmetry. As it cannot interact with such states, the surface state remains localized along \mathbf{J} - \mathbf{M} below the Fermi energy. We note that at \mathbf{J} the energy of the localized state of the strained Al(001) surface is about $E_F - 1.0 \text{ eV}$, i.e., $\sim 0.8 \text{ eV}$ smaller than the energy of the Al/GaAs(001) interface state.

The isolated, As-terminated GaAs(001) slab is artificial since the ideal, unreconstructed (001) surface of GaAs is metallic and unstable^{19,20} against surface reconstructions. For this ideal system, we obtain dangling- and bridge-bond surface states with energies within the semiconductor band gap which are comparable to those obtained in previous work.²¹ The dangling-bond surface state at \mathbf{J} has the full (Γ_1) symmetry of C_{2v} ,¹³ i.e., the same symmetry as the interface state shown in Fig. 4, while the bridge-bond state has a different (Γ_2) symmetry.

We have further examined the energy-band structure of the Al/GaAs(001) superlattice as a function of the interfacial distance d . Figure 7 shows the energy as a function of d of the electronic states at the \mathbf{J} point, which are close to the Fermi energy and have Γ_1 symmetry. The figure also indicates the calculated position of the conduction and valence PBS edges of the semiconductor as well as the stomach gap of Al bulk states with even symmetry at \mathbf{J} . Solid lines indicate localized states, while dotted lines indicate resonances.

For $d = 15a_0$, we recover the surface states of the isolated, strained Al(001) surface and of the unreconstructed, As-terminated GaAs(001) surface. The dangling-bond surface state of the latter surface occurs at $E_F - 0.3 \text{ eV}$. Furthermore, two localized Al surface states occur at about $E_F - 0.9 \text{ eV}$. It has to be noted, that the tetragonal supercell corresponds to

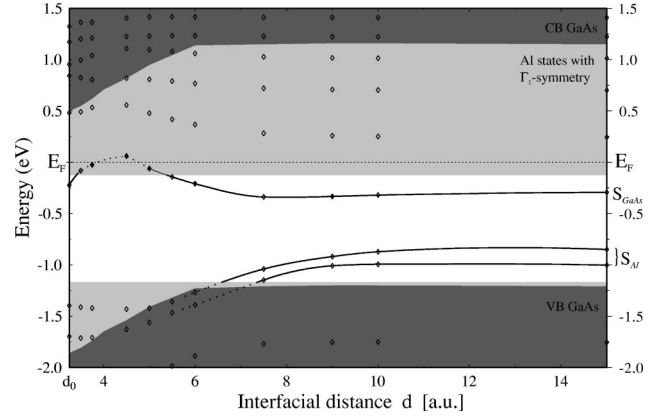


FIG. 7. Energy levels of the electron states of the Al/GaAs(001) superlattice at the \mathbf{J} point of the Brillouin zone as a function of interfacial separation between GaAs and Al slabs. Localized (solid) and resonant (dashed) states with Γ_1 symmetry are represented. Diamonds indicate calculated levels of the superlattice. Light gray areas indicate the band energies of bulk Al states with Γ_1 symmetry. Dark gray areas show bulk GaAs conduction- and valence-band energies.

an Al(001) $c2 \times 2$ surface, with two atoms in the unit cell, and therefore two surface states occur. Due to the finite size of the Al slab, these surface states interact and their energies split. This splitting is 0.15 eV (0.03 eV) for an Al slab consisting of 23 (41) layers.

Reducing the interfacial distance, the Al surface states interact with the dangling-bond surface state of the semiconductor resulting in a level repulsion. As a consequence, for interfacial distances smaller than $9a_0$, Al/GaAs interface states are a superposition of these two types of states. Decreasing further the interfacial distance to about $d = 7a_0$, the lower interface states leave the stomach gap of the Al bulk states with even symmetry, enter into the continuum, and delocalize.

For interfacial distances less than $5.5a_0$, the upper interface state raises in energy with respect to the Fermi energy, crosses the upper edge of the stomach gap of even bulk Al states, and enters the continuum. For interfacial distances smaller than $d = 3.5a_0$, the upper interface state lowers in energy, reenters the stomach gap, and relocalizes. The latter behavior is observed when the interface state is approaching the GaAs conduction PBS edge, whose energy decreases monotonously with respect to E_F for $d < 6a_0$. The behavior of the upper interface state for small values of d , together with the monotonic decrease of the GaAs conduction band, suggests a repulsion of the interface state from the semiconductor conduction-band edge at \mathbf{J} .

The above picture, including the level repulsion, is supported by a study of the changes taking place in the probability density of the upper interface state as a function of interfacial distance. Figure 8 shows contour plots of the probability density in the supercell basal plane for several values of d as well as the corresponding macroscopic average of the probability density along the growth axis, which yields a measure of the localization at the interface.

For $d \geq 9a_0$ [see Fig. 8(a)], we recover the probability

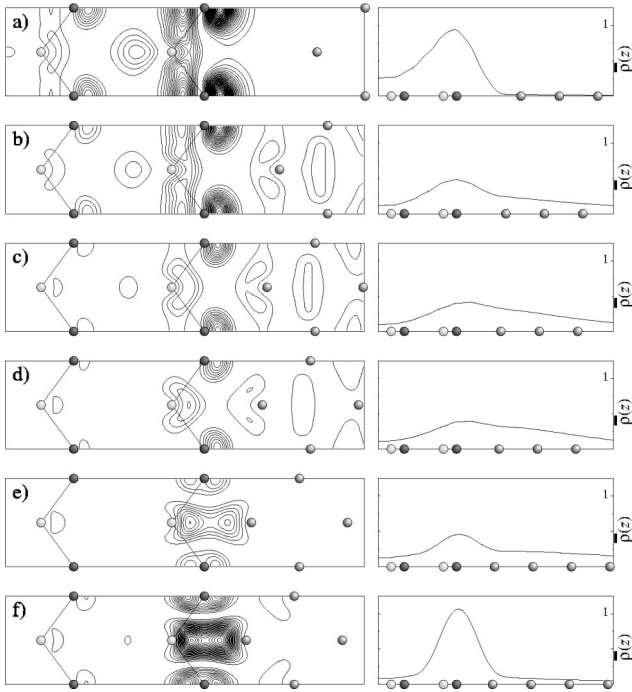


FIG. 8. Contour plot (left panel) and macroscopic planar average $\bar{p}(z)$ (right panel) of the probability density of the Al/GaAs(001) interface state at \mathbf{J} for selected values of the interfacial distance d : $9a_0$ (a), $6a_0$ (b), $5a_0$ (c), $4.5a_0$ (d), $3.75a_0$ (e), and $3.25a_0$ (f). Contour spacing is $1 \times 10^{-3} e/a_0^3$. Units of $\bar{p}(z)$ are $1 \times 10^{-4} e/a_0$.

density of the localized dangling-bond surface state of GaAs(001). For $d=6a_0$ [Fig. 8(b)], the interface state is a superposition of the GaAs dangling-bond and Al surface states. At $d=5a_0$ [Fig. 8(c)], a Ga-related feature appears with maximal probability density in the direction of the Al surface atom. The presence of this feature is ascribed to the interaction of the interface state with low-energy conduction-band states of GaAs at \mathbf{J} (see below). We note that the localization of the interface state at the junction reduces considerably at such intermediate distances ($5a_0$, $4.5a_0$) [Fig. 8(c, d)], when the interface state has left the stomach gap to enter the continuum of Al even states and to become a resonance. The formation of the bondinglike structure between the outermost Ga cations of the semiconductor and the interfacial Al atoms for $d \leq 3.75a_0$ [see Fig. 8(e)] gives rise to the dominant feature of the localized interface state found at $d = 3.25a_0$ [Fig. 8(f)].

The origin of the Ga-related feature was addressed by examining the probability density of the lowest GaAs conduction states that contribute to the PBS at \mathbf{J} . In Fig. 9, we show the probability density of the GaAs bulk state with Γ_1 symmetry (in the bulk tetragonal cell), which corresponds to the minimum of the conduction PBS at \mathbf{J} . This state derives from Bloch states of the \mathbf{L} conduction-band minima of the GaAs 3D-BZ, which are projected onto \mathbf{J} in two dimensions. The probability density of this state is large near the Ga atom, with a structure which is similar to that of the Ga-related feature involved in the formation of the Al-Ga intermetallic bonding structure in Fig. 8. We conclude, thus, that

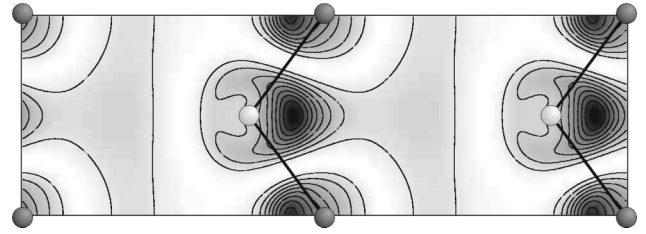


FIG. 9. Contour plot of the probability density of the bulk GaAs state with Γ_1 symmetry which corresponds to the conduction-band minimum of the PBS at \mathbf{J} . This state derives from GaAs Bloch states at the \mathbf{L} conduction-band minima of the 3D-BZ. Contour spacing is $3.5 \times 10^{-3} e/a_0^3$.

the decrease in energy of the interface state for small d , which corresponds to the formation of the intermetallic bonding structure, derives from an interaction with the continuum of GaAs bulk states near the conduction-band minimum at \mathbf{L} .

Calculations for the Al/GaAs(001) superlattice have also been performed with pseudopotentials, where d electrons are treated as valence electrons. The existence of the localized interface state at \mathbf{J} and its nature are fully confirmed by these results.

Presently, similar calculations are under way for the Al/AlAs(001) system.²² The preliminary results indicate the existence of interface resonance states in the semiconductor gap near the \mathbf{J} point of the BZ. The electronic structure of AlAs is somewhat different from that of GaAs, in particular, the conduction-band edge at \mathbf{J} occurs at a higher energy. Due to this, the repulsion near the equilibrium distance of the upper interface state with conduction-band states is weaker and the interface state occurs at higher energy. In this case, the interface state is degenerate of bulk Al states with even symmetry. Consequently, it is not localized, rather it is a strong resonance with similar charge-density distribution at the interface, which resembles that of the localized state studied in this work. Therefore, the difference in semiconductor polarity between GaAs and AlAs has thus quantitative, but no qualitative influence on this phenomenon.

IV. SUMMARY AND OUTLOOK

By means of first-principles calculations, we have studied the nature of the electronic states with energy within the semiconductor band gap at abrupt, As-terminated, epitaxial Al/GaAs(001) junctions. The results indicate the existence of electronic states near the Fermi energy which exhibit a high probability density at the interface. In particular, we find a localized interface state at the \mathbf{J} point of the interface Brillouin zone. These states have an unexpected nature, namely, an intermetallic, bondinglike character between outermost Al atoms from the metal and Ga atoms from the second semiconductor layer across the interface.

The mechanism responsible for the formation of the localized interface state at \mathbf{J} has been identified by studying the electronic energies as a function of the interfacial distance. We have found that the interface state derives from an inter-

action between localized states of the isolated Al(001) surface and GaAs bulk conduction band-edge states, mediated by dangling-bond surface states of the isolated, unreconstructed GaAs(001) surface. The interaction process identified in this work is a robust mechanism, which may be expected to occur also in other systems. Indeed, preliminary results for isomorphic Al/AlAs(001) indicate that similar interface states exist within this system.

It remains to be verified if similar interface states related to preexisting surface states occur also in other systems, e.g., for other polar interface orientations and for other materials.

The predicted localized interface states should be accessible to experimental measurements, e.g., spectroscopic investigations at low coverage or possibly scanning tunneling microscope techniques at cleaved samples.

ACKNOWLEDGMENTS

We acknowledge support by the Swiss National Foundation under Grant No. 20-65150.01. Computations were performed at the Computer Center of the EPFL and at the CSCS in Manno.

-
- ¹*Electronic Structure of Metal-Semiconductor Contacts*, edited by W. Mönch (Kluwer Academic, London, 1990).
- ²*Metal-Semiconductor Interfaces*, edited by A. Hiraki (Ohmsha, Tokyo, Japan, 1995).
- ³J. Bardi, N. Binggeli, and A. Baldereschi, *Phys. Rev. B* **61**, 5416 (2000).
- ⁴P. Revva, J.M. Langer, M. Missous, and A.R. Peaker, *J. Appl. Phys.* **741**, 416 (1993).
- ⁵L. Dobaczewski, J.M. Langer, and M. Missous, *Acta Phys. Pol. A* **84**, 741 (1993); *Proceedings of the XXII International Conference of Physics and Semiconductors*, edited by D.J. Lockwood (World Scientific, Singapore, 1994), p. 588.
- ⁶J. Bardi, N. Binggeli, and A. Baldereschi, *Phys. Rev. B* **54**, R11 102 (1996).
- ⁷N. Troullier and J.L. Martins, *Phys. Rev. B* **43**, 1993 (1991).
- ⁸L. Kleinman and D.M. Bylander, *Phys. Rev. Lett.* **48**, 1425 (1982).
- ⁹M. Peressi, N. Binggeli, and A. Baldereschi, *J. Phys. D: Appl. Phys.* **31**, 1273 (1998), and references therein.
- ¹⁰J. Bardi, N. Binggeli, and A. Baldereschi, *Phys. Rev. B* **59**, 8054 (1999).
- ¹¹A.Y. Cho and P.D. Dernier, *J. Appl. Phys.* **49**, 3328 (1978).
- ¹²G. Landgren, R. Ludeke, and C. Serrano, *J. Cryst. Growth* **60**, 3938 (1982).
- ¹³G. Koster, J. Dimmock, R. Wheeler, and H. Statz, *Properties of the Thirty-Two Point Groups* (MIT Press, Cambridge, 1960).
- ¹⁴H. Monkhorst and J. Pack, *Phys. Rev. B* **13**, 5188 (1976).
- ¹⁵C.L. Fu and K.M. Ho, *Phys. Rev. B* **28**, 5480 (1983).
- ¹⁶J. Tersoff, *Phys. Rev. B* **32**, 6968 (1985).
- ¹⁷A. Zangwil, *Physics at Surfaces* (Cambridge University Press, Cambridge, 1988).
- ¹⁸E. Caruthers, L. Kleinmann, and G. Alldredge, *Phys. Rev. B* **8**, 4570 (1973).
- ¹⁹J. Appelbaum and D. Hamann, *Phys. Rev. B* **10**, 4973 (1974).
- ²⁰J. Appelbaum, G.A. Baraff, and D. Hamann, *Phys. Rev. B* **14**, 1623 (1976).
- ²¹I. Ivanov, A. Mazur, and J. Pollmann, *Surf. Sci.* **92**, 365 (1980).
- ²²T. Maxisch, N. Binggeli, and A. Baldereschi (unpublished).